AIAA JOURNAL
Vol. 31, No. 11, November 1993

# Three-Dimensional Velocity Field in a Compressible Mixing Layer

Mark R. Gruber*
*Wright Laboratory, Wright-Patterson AFB, Ohio 45433*
Nathan L. Messersmith†
*Purdue University, West Lafayette, Indiana 47907*
and
J. Craig Dutton‡
*University of Illinois at Urbana-Champaign, Urbana, Illinois 61801*

**A turbulent, compressible mixing layer with a relative Mach number of 1.59 has been investigated experimentally using a two-component laser Doppler velocimeter system. Two sets of profiles were obtained at each streamwise measurement location to compile the streamwise, transverse, and spanwise turbulence statistics. Results from the fully developed region of the mixing layer showed similar peak values of streamwise and spanwise turbulence intensities along with reduced peak values of transverse turbulence intensity, normalized primary Reynolds shear stress, and normalized turbulent kinetic energy in comparison to the respective quantities from incompressible shear layers. Because the Reynolds normal stress ratio $\sigma_v/\sigma_w$ was found to decrease with increasing relative Mach number, it is concluded that the spanwise component of the mixing layer turbulence becomes more important as compressibility is increased. In addition, various turbulence profiles demonstrated a reduction of lateral extent on the high speed side of the mixing layer as compared to profiles in incompressible mixing layers.**

## Nomenclature

$a$ = speed of sound
$b$ = mixing layer thickness, distance between transverse locations where $U = U_1 - 0.1(\Delta U)$ and $U = U_2 + 0.1(\Delta U)$
$M$ = Mach number
$M_c$ = convective Mach number $= \Delta U/(a_1 + a_2)$
$M_r$ = relative Mach number $= 2\Delta U/(a_1 + a_2)$
$P$ = static pressure
$P_t$ = total pressure
$q^2$ = turbulent kinetic energy $= \langle u^2 \rangle + \langle v^2 \rangle + \langle w^2 \rangle$
$r$ = velocity ratio $= U_2/U_1$
$Re$ = unit Reynolds number $= (\rho_1 + \rho_2)\Delta U/(\mu_1 + \mu_2)$
$Re_b$ = Reynolds number based on shear layer width $= b(\rho_1 + \rho_2)\Delta U/(\mu_1 + \mu_2)$
$s$ = density ratio $= \rho_2/\rho_1$
$T$ = static temperature
$T_t$ = total temperature
$u$ = streamwise velocity fluctuation
$u_\tau$ = friction velocity
$U$ = local mean freestream velocity
$\Delta U$ = freestream velocity difference $= U_1 - U_2$
$v$ = transverse velocity fluctuation
$w$ = spanwise velocity fluctuation
$x$ = streamwise coordinate
$x_0$ = virtual origin
$y$ = transverse coordinate
$y_0$ = mixing layer centerline
$\delta$ = boundary-layer thickness (transverse location where velocity is 99.5% freestream velocity)
$\delta^*$ = compressible boundary-layer displacement thickness
$\eta$ = similarity variable $= (y - y_0)/b$
$\theta$ = compressible boundary-layer momentum thickness
$\lambda$ = velocity parameter $= (1 - r)/(1 + r)$
$\lambda_s$ = velocity-density parameter $= (1 - r)(1 + s^{1/2})/[2(1 + rs^{1/2})]$
$\mu$ = dynamic viscosity
$\rho$ = density
$\sigma$ = standard deviation
$\langle\,\rangle$ = ensemble average

*Subscripts*

$c$ = compressible
$i$ = incompressible
max = maximum value
mean = mean value within the mixing layer

Received April 8, 1992; presented as Paper 92-3544 at the AIAA/SAE/ASME/ASEE 28th Joint Propulsion Conference, Nashville, TN, July 6–8, 1992; revision received Dec. 28, 1992; accepted for publication Jan. 8, 1993. 

*Aerospace Engineer, Advanced Propulsion Division, Aero-Propulsion and Power Laboratory. Member AIAA.
†Assistant Professor, School of Aeronautics and Astronautics. Member AIAA.
‡Professor, Department of Mechanical and Industrial Engineering. Associate Fellow AIAA.

## Introduction

THE study of compressible mixing layers has received considerable attention lately in relation to hypersonic aircraft concepts that will require an air-breathing propulsion system. Critical to the performance of such a propulsion system are the entrainment, mixing, and combustion processes carried out within the mixing layer created at the interface between the high-speed fuel and airstreams in the combustor. Compressible mixing layers are also fundamental to many other practical devices such as supersonic ejectors, chemical and gas dynamic lasers, missile and projectile base flows, etc.

Incompressible mixing layers have been thoroughly investigated by a number of researchers.[1–4] These studies have produced information about the mixing layer growth rates, turbulence statistics, and structural organization. Not until more recently, however, has the study of compressible mixing layers come into its own. Many investigators have documented the relatively slow growth of the compressible mixing layer as compared with an incompressible mixing layer at the same

freestream velocity and density ratios.[5-9] Furthermore, experimental results from the two-dimensional laser Doppler velocimeter (LDV) investigations (streamwise and transverse velocity components) of Goebel and Dutton[6] and Elliott and Samimy[7] have documented a significant reduction of the transverse turbulence intensity ($\sigma_v/\Delta U$) and normalized primary Reynolds shear stress [$-\langle uv\rangle/(\Delta U^2)$] with increasing compressibility. These studies have also produced somewhat different results concerning the trend of the streamwise turbulence intensity ($\sigma_u/\Delta U$); Goebel and Dutton[6] found nearly constant values with increasing compressibility, whereas Elliott and Samimy[7] found a reduction similar to the transverse component. In addition to these, experiments employing planar visualization techniques have been conducted with the intent of examining the organized structure within compressible mixing layers.[8,9] Results of these experiments have shown that increases in compressibility produce a large scale turbulence structure that is reoriented in a direction more oblique to the streamwise flow direction. Other experiments using spatial correlations of pressure measurements have shown similar trends in that a less organized, more oblique structure develops with increasing compressibility.[10,11] Computations by Sandham and Reynolds,[12] Leep et al.,[13] and others also suggest an increase in the importance of three-dimensional instabilities at higher levels of compressibility.

To quantify the effects of compressibility, many researchers use the convective Mach number first proposed by Bogdanoff.[14] However, numerous studies have documented large structure convection velocities that are substantially different from those predicted using the convective Mach number analysis.[15,16] Because of the apparent problems associated with this parameter, the relative Mach number, suggested by Ragab and Wu,[17] and defined as

$$M_r = 2\Delta U/(a_1 + a_2) \tag{1}$$

will be used throughout this investigation as the parameter describing the compressibility of two-stream mixing layers.

The primary objective of this work is to report turbulence statistics for all three velocity components in a compressible mixing layer, as an extension of the previous two-dimensional measurements of Goebel and Dutton[6] and Elliott and Samimy.[7] Because the recent visualization studies cited previously have shown the mixing layer structure to become increasingly three dimensional (i.e., more obliquely oriented large structures) at higher levels of compressibility, it is important to report the previously unmeasured spanwise velocity statistics as well. Also, because all three Reynolds normal stresses are directly measured, the turbulent kinetic energy profile in a fully developed compressible mixing layer can be presented, which is of direct interest to turbulence modelers. Finally, the current measurements provide additional data regarding the trend of the streamwise turbulence intensity, and therefore normal stress anisotropy, with increasing compressibility, for which the previous measurements of Goebel and Dutton[6] and Elliott and Samimy[7] show somewhat different results.

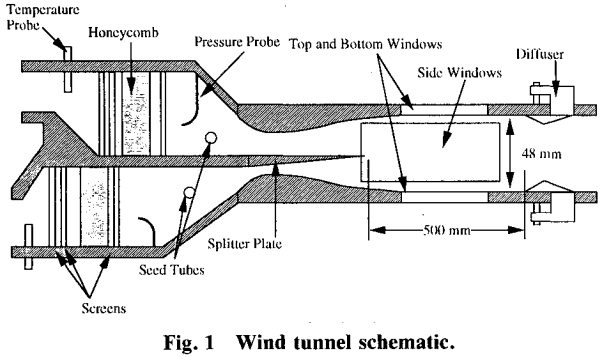


**Fig. 1 Wind tunnel schematic.**

## Experimental Facility and Instrumentation

### Test Section

The dual stream supersonic mixing layer wind tunnel used in this study is located at the University of Illinois and is illustrated schematically in Fig. 1. High pressure air was available for the experiments from an intermediate storage tank farm, which was fed by two compressors. Two airstreams supplied the test section, and the conditions of each stream could be controlled independently. Conditioning of the two airstreams was accomplished in the wind tunnel plenum chambers using a length of honeycomb placed between three mesh screens. To achieve the desired test conditions, a pair of supersonic half nozzles with nominal Mach numbers 2.5 (primary, top stream) and 1.4 (secondary, bottom stream) was used. For the present investigation, the secondary nozzle was run subsonically to increase the velocity difference, and therefore the relative Mach number, of the mixing layer. These nozzles were separated by a thin splitter plate, downstream of which the two streams were allowed to interact and form the mixing layer in the 500-mm-long test section. Optical access to the flow was achieved through the use of two window configurations. First, quartz windows could be mounted in each side wall of the test section allowing access for LDV measurements of the streamwise and transverse components of velocity. The second arrangement involved glass windows mounted in the top and bottom walls of the test section allowing access for LDV measurements of the streamwise and spanwise components of velocity.

### Laser Doppler Velocimeter System

A two-color, two-component dual-beam Thermal Systems Incorporated (TSI) LDV system was used for these experiments. Specifically, the blue (488 nm) and green (514.5 nm) lines of a 4 W argon-ion laser were used to form the two-component measurement volume. Bragg cell frequency shifting of 40 MHz was used on one beam of each pair for all of the two-component measurements to reduce the effects of fringe

**Table 1 Experimental conditions, mixing layer parameters, and results**

| Quantity | Value |
|---|---|
| $r = U_2/U_1$ | 0.17 |
| $\lambda = (1-r)/(1+r)$ | 0.71 |
| $s = \rho_2/\rho_1$ | 0.46 |
| $\lambda_s = (1-r)(1+s^{1/2})/[2(1+rs^{1/2})]$ | 0.63 |
| $M_r = 2\Delta U/(a_1+a_2)$ | 1.59 |
| $M_c = \Delta U/(a_1+a_2)$ | 0.80 |
| $Re = (\rho_1+\rho_2)\Delta U/(\mu_1+\mu_2)$, $10^6$/m | 26.2 |
| $P_{t1}$, $P_{t2}$, kPa | 552, 43.4 |
| $T_{t1}$, $T_{t2}$, K | 279, 289 |
| $P_1$, $P_2$, kPa | 40.3, 40.3 |
| $U_1$, $U_2$, m/s | 543, 91.2 |
| $T_1$, $T_2$, K | 132, 285 |
| $a_1$, $a_2$, m/s | 230, 338 |
| $M_1$, $M_2$ | 2.36, 0.27 |
| $\rho_1$, $\rho_2$, kg/m$^3$ | 1.06, 0.49 |
| $\mu_1$, $\mu_2$, $10^{-6}$ Pa-s | 9.10, 17.7 |
| $\delta_1$, $\delta_2$, mm | 1.6, 1.5 |
| $\delta_1^*$, $\delta_2^*$, mm | 0.21, 0.12 |
| $\theta_1$, $\theta_2$, mm | 0.061, 0.082 |
| $u_{\tau 1}$, $u_{\tau 2}$, m/s | 27, 8.0 |
| $(db/dx)_c$ | 0.052 |
| $x_0$, mm | −28 |
| $(db/dx)_c/(db/dx)_i$ | 0.50 |
| $(\sigma_u/\Delta U)_{max}$ | 0.17 |
| $(\sigma_v/\Delta U)_{max}$ | 0.072 |
| $(\sigma_w/\Delta U)_{max}$ | 0.13 |
| $\langle q^2\rangle/(\Delta U^2)_{max}$ | 0.048 |
| $(\sigma_u/\sigma_v)_{max}$ | 2.35 |
| $(\sigma_u/\sigma_w)_{max}$ | 1.32 |
| $(\sigma_v/\sigma_w)_{max}$ | 0.55 |
| $[-\langle uv\rangle/(\Delta U)^2]_{max}$ | 0.0065 |
| $[-\langle uv\rangle/\sigma_u\sigma_v]_{mean}$ | 0.48 |

blindness. The entire LDV system was translated in the streamwise and transverse directions using a traversing table controlled with the serial interface of the Macintosh II data acquisition computer.[18] In addition to the existing table, a special receiving optics table was constructed for the streamwise/spanwise measurements that allowed mounting of the receiving optics above the test section and 10 deg off the forward scatter axis. TSI frequency counters were used to process the signals received from the photomultiplier tubes. For these two-component measurements, the coincidence window on the counters was set to 2 $\mu$s. The data processed by the frequency counters were acquired and analyzed using the Macintosh II and a National Instruments parallel interface board. Both the primary and secondary streams were independently seeded with silicone oil droplets from a TSI six-jet atomizer. This seeder was characterized by Bloomberg[19] as producing polydispersed particles of nominal mean diameter of 0.8 $\mu$m.

Velocity profiles were obtained in the transverse direction across the mixing layer at 13 streamwise locations for each LDV configuration starting at 50 mm downstream of the splitter splate tip and continuing every 10 mm to 170 mm downstream of the tip. Boundary-layer profiles were also obtained at a streamwise location 2 mm upstream of the tip using a one-component LDV arrangement that measured the streamwise velocity. All of the velocity profiles presented here have been corrected for fringe bias according to the analysis of Buchhave.[20] Correction for velocity bias was also performed using an inverse velocity magnitude weighting factor, but the resulting profiles demonstrated no appreciable difference when compared to the uncorrected profiles. For this reason, no velocity bias correction has been used on the data presented herein. Further detail concerning the facility, LDV system, procedures, and measurement uncertainties may be found in Gruber.[21]

## Experimental Results

### Experimental Conditions

The operating conditions and mixing layer parameters of the present study are listed in Table 1. The mixing layer examined here has a relative Mach number of 1.59. This condition was chosen since it falls within the region of moderate compressibility as defined by Papamoschou and Roshko[5] and, according to Sandham and Reynolds,[12] it should display a significant increase in large structure three-dimensionality over incompressible cases due to the more dominant role played by oblique instability waves. The unit Reynolds number for this compressible mixing layer was calculated to be $26.2 \times 10^6$ m$^{-1}$ using the freestream velocity difference and the average of the freestream densities and viscosities.

The state of the incoming boundary layers is important to quantify because these boundary layers provide the initial condition for the growth of the mixing layer at the splitter plate tip. Measured turbulence intensities indicated that both boundary layers were turbulent, as expected for the present operating conditions. The experimental data were least-squares fit using the compressible, turbulent boundary-layer profile equation of Sun and Childs.[22] All of the various integral parameters determined from the least-squares fit are given in Table 1 for each boundary layer.

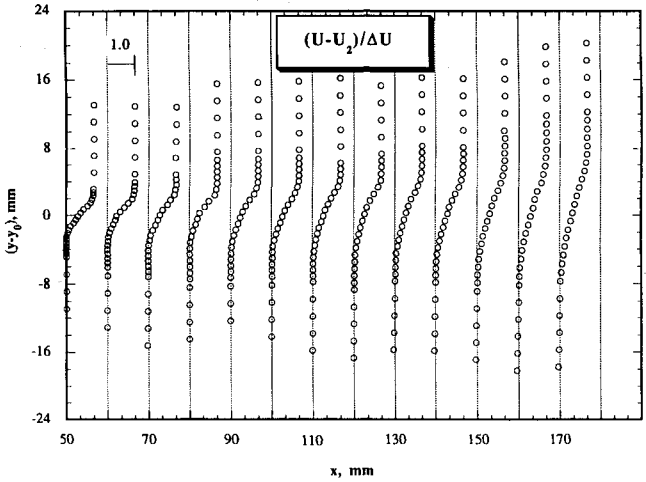


**Fig. 2 Development of normalized mean streamwise velocity.**

### Mixing Layer Development and Growth Rate

Spatial development of the normalized mean streamwise velocity obtained from the first LDV measurement configuration (streamwise-transverse) is presented in Fig. 2. The figure plots the quantity $(U - U_2)/\Delta U$ on a grid showing the transverse and streamwise locations of the data. The transverse coordinate is shifted to the mixing layer center by subtracting the mixing layer centerline location $y_0$, defined as $0.5(y_{90} + y_{10})$, from the actual transverse measurement location. The dashed lines show the individual streamwise measurement locations and also represent the locations where the plotted quantity is zero. Finally, the scale for the plotted quantity is included at the upper left of the figure. The mixing layer is clearly evident in the figure as the region between the uniform freestreams. Because none of the profiles showed evidence of a velocity deficit, the growth region was taken to be the region between 50 and 170 mm downstream of the splitter plate tip. The Reynolds number based on mixing layer thickness was calculated to be $1.12 \times 10^5$ at $x = 50$ mm.

The mixing layer growth rate was obtained using the 10% $\Delta U$ thickness definition in the growth region, where $\Delta U$ was calculated as the difference between the local primary and secondary freestream velocities at each streamwise measurement location. Both the growth rate $(db/dx)_c = 0.052$ and the virtual origin $x_0 = -28$ mm are included in Table 1. Also included in the table is the compressible mixing layer growth rate normalized by the incompressible mixing layer growth rate, which is calculated at the same freestream velocity and density ratios and given by[18]

$$(db/dx)_i = 0.165\lambda_s = 0.104 \tag{2}$$

The normalized growth rate is found to have a value of 0.50 indicating that the compressible mixing layer studied suffers a greatly reduced growth rate compared with its incompressible counterpart. This value for the normalized growth rate is also consistent with previous LDV studies of Goebel and Dutton[6] and Eliott and Samimy,[7] which together with the results of other workers demonstrate a monotonically decreasing normalized growth rate with increasing compressibility.

From spatial development plots of the streamwise, transverse, and spanwise turbulence intensities, $\sigma_u/\Delta U$, $\sigma_v/\Delta U$, and $\sigma_w/\Delta U$, respectively, the peak intensity values appear to be relatively constant downstream of about $x = 70$ mm where the local Reynolds number based on mixing layer thickness was calculated to be $Re_b = 1.35 \times 10^5$. The development of the normalized primary Reynolds shear stress $-\langle uv \rangle/(\Delta U)^2$ appears to exhibit constant peak values downstream of about 100 mm of the splitter plate tip, where the local Reynolds number is $Re_b = 1.76 \times 10^5$. Goebel and Dutton[6] suggested that a value of $Re_b$ on the order of $1 \times 10^5$ is required for full development of the mean and turbulent velocity fields to be reached. As just noted, the present mixing layer attains a value of $Re_b = 1.76 \times 10^5$ by 100 mm downstream of the splitter plate tip where the peak turbulence quantities have become constant, whereas the maximum value of $Re_b$ for the current investigation has been calculated to be $2.76 \times 10^5$. Therefore, from examination of the spatial development of the various quantities presented here and in more detail in Ref. 21, a fully developed condition certainly seems to exist for these results well upstream of the last streamwise measurement location.

### Mixing Layer Similarity Averages

Figures 3–7 illustrate the results of averaging the profiles for various mean and turbulent quantities from within the region

of the mixing layer found to be fully developed. These profiles have been used to document the peak values of the various turbulence quantities; Table 1 summarizes the most important of these results.

The normalized mean streamwise velocity is shown in Fig. 3. As expected, the profile shows a strong resemblance to the error function profile that results from Göertler's analysis of the incompressible mixing layer.[23] This profile also compares well with the results of the recent LDV investigations of both Goebel and Dutton[6] and Elliott and Samimy.[7]

The averaged turbulence intensity profiles are shown in Fig. 4. The peak value of streamwise turbulence intensity within the mixing layer is observed to be about 0.17. This value agrees well with the results of Goebel and Dutton,[6] which indicate that the streamwise turbulence intensity remains relatively constant (at a value of approximately $\sigma_u/\Delta U = 0.18$) with increasing relative Mach number. On the other hand, the peak streamwise turbulence intensities measured by Elliott and Samimy[7] show a relatively small but distinct reduction with increasing compressibility over a narrower range of $M_r$ than that investigated by Goebel and Dutton.[6] The streamwise turbulence intensity profile also seems to suggest a reduction of lateral extent on the high-speed side of the mixing layer, which is consistent with the findings of Elliott and Samimy.[7] This reduction is demonstrated by the tendency of the streamwise turbulence intensity within the mixing layer to decay very quickly to the freestream value on the high-speed side, whereas the same decay occurs more gradually on the low-speed side.

The transverse turbulence intensity profile presented in Fig. 4 also suggests a reduction of lateral extent on the high-speed side in the same manner as the streamwise component. A peak value of about 0.072 is observed. Compared to the incompressible data,[2-4] $(\sigma_v/\Delta U)_i = 0.13$, a substantial reduction in this quantity is observed as compressibility increases. Combining the streamwise and transverse turbulence intensity results from the previous studies produces two different trends concerning the magnitude of the peak normal stress anisotropy $\sigma_u/\sigma_v$: that of Goebel and Dutton[6] indicates an increase with compressibility whereas that of Elliott and Samimy[7] shows relatively constant values with increasing compressibility. The present data support the former of these trends with a value of $\sigma_u/\sigma_v = 2.35$ as compared with the incompressible value of $(\sigma_u/\sigma_v)_i = 1.38$. Therefore, a major effect of compressibility on the mixing layer turbulence is the suppression of the transverse velocity fluctuations resulting in an increasingly anisotropic structure, in terms of the streamwise and transverse components.

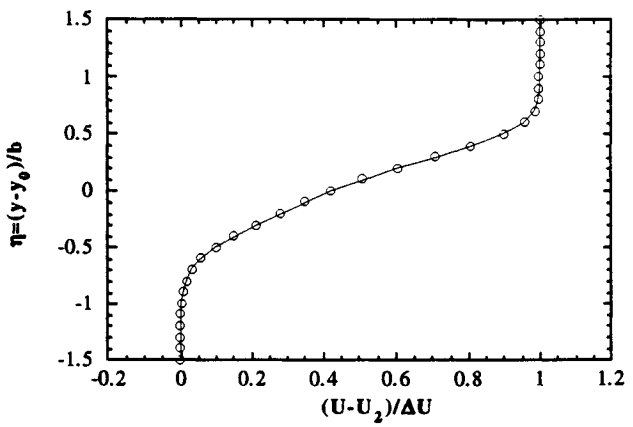


Fig. 3 Similarity of normalized mean streamwise velocity.

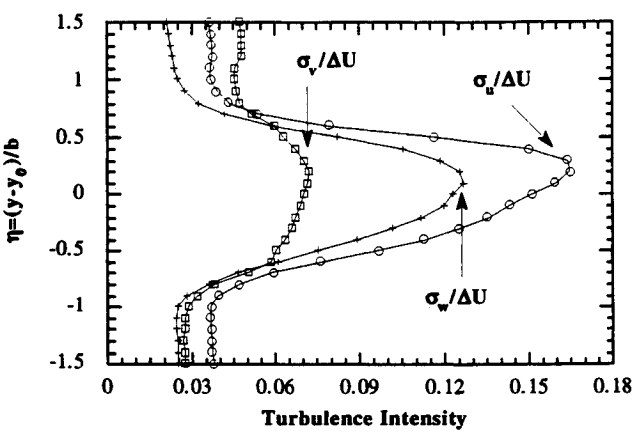


Fig. 4 Similarity of turbulence intensity components.

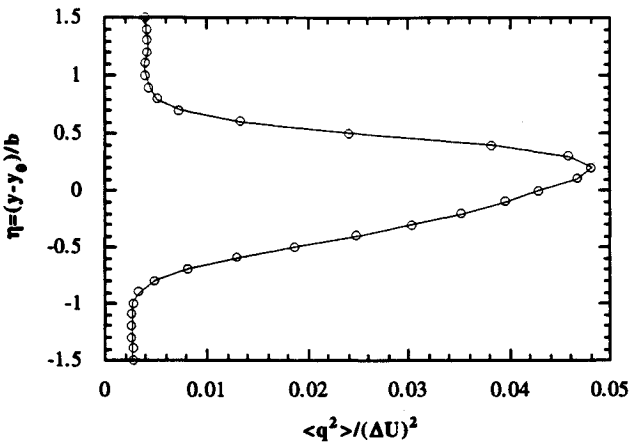


Fig. 5 Similarity of normalized turbulent kinetic energy.

Figure 4 also shows the averaged spanwise turbulence intensity profile for the present case. In contrast to the other two turbulence intensity plots, the spanwise profile appears more symmetrical, i.e., there appears to be a smaller reduction in lateral extent on the high-speed side of the mixing layer. This profile also attains a peak value of about 0.13, which is comparable to the value measured in incompressible mixing layers.[2-4] Therefore, just as for the peak streamwise turbulence intensity, this quantity shows no significant reduction with increased compressibility. However, the peak $\sigma_v/\sigma_w$ normal stress anisotropy shows a reduction compared with the available incompressible data. For the present mixing layer, a peak value of $\sigma_v/\sigma_w = 0.55$ is observed. This quantity represents a direct measure of the relative importance of the transverse and spanwise Reynolds normal stresses. For the incompressible mixing layer, the peak value of $\sigma_v/\sigma_w$ is roughly unity,[2-4] indicating equality of the magnitude of the transverse and spanwise velocity fluctuations. The reduction of this quantity with increasing compressibility is indicative of the mixing layer structure becoming more dependent on three-dimensional disturbances with a concomitant increase in the magnitude of spanwise as compared to transverse velocity fluctuations. This observation agrees in concept with the recent planar visualization and computational results of Clemens,[8] Messersmith,[9] and Sandham and Reynolds[12] to name a few. The other normal stress anisotropy term $\sigma_u/\sigma_w$ is computed to have a peak value of roughly 1.32 within the mixing layer. Comparison to the incompressible data suggests that this normal stress anisotropy remains relatively constant with increasing compressibility.

Knowledge of the three turbulence intensities allows the calculation of the normalized turbulent kinetic energy $\langle q^2\rangle/(\Delta U)^2$ by simply summing the squares of each component (i.e., sum of the normalized Reynolds normal stresses). As mentioned, this result is of direct interest to those turbulence modelers interested in computing compressible shear flows. Figure 5 presents the results of this calculation using the three averaged turbulence intensity profiles. The peak value of this quantity for the present flow conditions is about 0.048 as

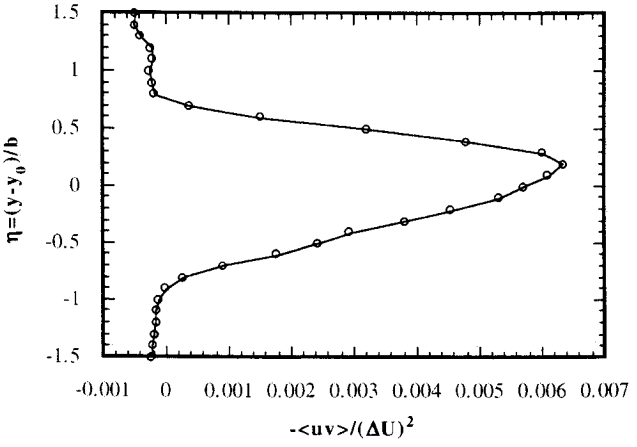


Fig. 6 Similarity of normalized primary Reynolds shear stress.

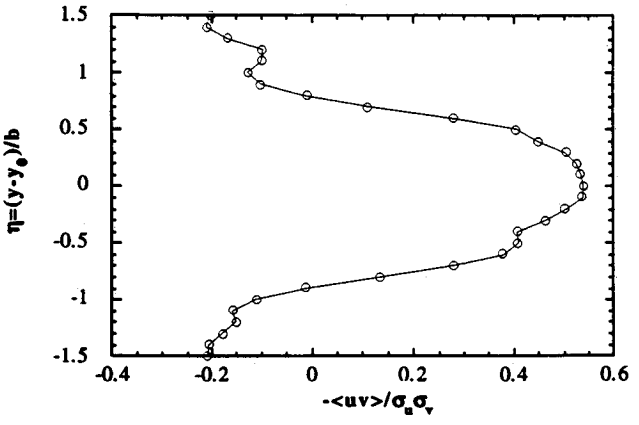


Fig. 7 Similarity of primary Reynolds shear stress correlation coefficient.

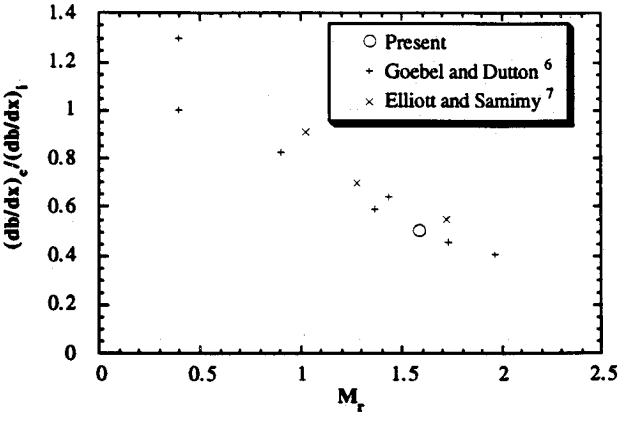


Fig. 8 Normalized growth rates from recent LDV investigations.

compared with a value of approximately 0.066 for incompressible mixing layers.[2-4] This reduction of roughly 27% is largely a function of the reduced transverse turbulence intensity, because the other two components have been shown to remain relatively constant with increasing relative Mach number.

The averaged normalized primary Reynolds shear stress profile $-\langle uv\rangle/(\Delta U)^2$ is presented in Fig. 6. The observed peak value for this compressibility condition is approximately 0.0065, which agrees very well with the trend of other data available[6,7] and is a substantial reduction compared with the incompressible value of 0.013.[18] Because this quantity represents the transverse transport of streamwise momentum, reductions in it certainly play a major role in the reduced rate of spread of compressible mixing layers as compared with their incompressible counterparts. The present profile also shows a reduction in lateral extent on the high-speed side of the mixing layer of the Reynolds stress. The primary Reynolds shear stress correlation coefficient $-\langle uv\rangle/\sigma_u\sigma_v$ is displayed in Fig. 7. It is observed that this quantity remains nearly constant across the central portion of the mixing layer, with a mean value in the mixing layer of about 0.48. The trend is in good agreement with the results obtained by other investigators[6,7] who also indicate that this correlation coefficient remains relatively constant across this region of the mixing layer and with changes in compressibility. The magnitude of the present quantity compares very favorably with those of the aforementioned authors who quote values of approximately 0.51 and 0.45, respectively.

### Compressibility Effects

To better examine the effects of compressibility on the mixing layer statistics, it is useful to normalize the various parameters by an appropriate value from incompressible studies, and plot the resulting quantity with increasing relative Mach number. Results from recent LDV investigations[6,7] have been compiled and added to the present results in Figs. 8-11. These plots illustrate the effects of increasing compressibility on mixing layer growth rate, streamwise and transverse turbulence intensity, and primary Reynolds shear stress. Normalizing values for the turbulence quantities have been obtained for incompressible shear layers as follows[2-4,18]: $(\sigma_u/\Delta U)_i = 0.18$, $(\sigma_v/\Delta U)_i = 0.13$, and $[-\langle uv\rangle/(\Delta U)^2]_i = 0.066$.

Figure 8 shows a reduction of normalized growth rate with increasing compressibility. All of the fully developed data (ignoring the "disturbed" case 1d of Goebel and Dutton[6]) are consistent, suggesting that the normalized growth rate decreases monotonically with increasing compressibility.

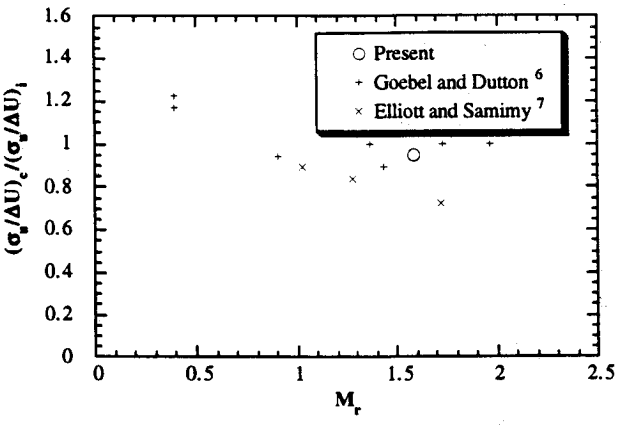


Fig. 9 Normalized streamwise turbulence intensities from recent LDV investigations.

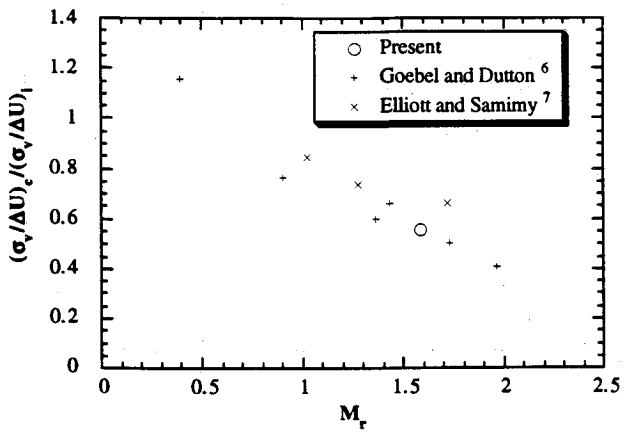


Fig. 10 Normalized transverse turbulence intensities from recent LDV investigations.

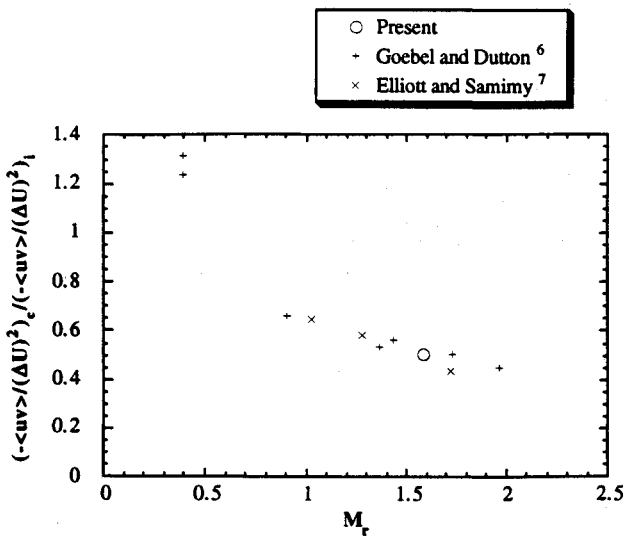


**Fig. 11 Normalized primary Reynolds shear stresses from recent LDV investigations.**

Comparison of the normalized peak streamwise turbulence intensities found in Fig. 9 shows two trends. The data of Goebel and Dutton[6] show a relatively constant level, whereas data from Elliott and Samimy[7] suggest a reduction with compressibility over a narrower range of $M_r$. The present data are more consistent with the former study, suggesting that the peak values of streamwise turbulence intensity remain nearly constant with increases in compressibility.

Examination of Fig. 10, which shows the trend of normalized peak transverse turbulence intensity with increasing $M_r$, leads to the conclusion that the transverse velocity fluctuations are consistently suppressed as the mixing layer becomes more compressible. Together with the constant streamwise turbulence intensity, the mixing layer therefore becomes increasingly anisotropic as relative Mach number increases.

Finally, Fig. 11 shows the trend of normalized peak primary Reynolds shear stress with increasing relative Mach number. Here again, a monotonic reduction is observed as compressibility increases. This is a direct result of suppressed transverse velocity fluctuations.

Because no measurements of spanwise turbulence intensity are available for compressible mixing layers outside of the present study, no plot is shown. However, comparing the results of the present study to incompressible data from the literature, the newly measured component of the turbulence field is found to have no reduction with increasing compressibility. Clearly, the turbulence structure of the mixing layer becomes more dependent on the spanwise turbulence level as compressibility increases due to the suppression of the transverse component.

## Summary and Conclusions

The first measurements of mean and turbulent velocity profiles of all three velocity components have been obtained from within the developing and fully developed regions of a turbulent, compressible mixing layer ($M_r = 1.59$). The results demonstrate that the peak streamwise turbulence intensity $\sigma_u/\Delta U$ remains relatively constant as compressibility increases, in agreement with Goebel and Dutton.[6] Peak values of transverse turbulence intensity $\sigma_v/\Delta U$, and normalized primary Reynolds shear stress $-\langle uv\rangle/(\Delta U)^2$, decrease with increasing compressibility like the normalized growth rate, implying that the primary effect of compressibility on the mixing layer is to suppress transverse velocity fluctuations. The peak spanwise turbulence intensity $\sigma_w/\Delta U$ remains relatively constant with increasing compressibility. Therefore, the Reynolds normal stress anisotropy defined as $\sigma_v/\sigma_w$ decreases with increasing relative Mach number due to the suppression of the transverse velocity fluctuations. This implies that an effect of compressibility on the mixing layer turbulence structure is a tendency toward more three-dimensional behavior (i.e., obliquely oriented large scale structures) with enhanced spanwise as compared to transverse velocity fluctuations. The peak normalized turbulent kinetic energy $\langle q^2\rangle/(\Delta U)^2$ decreases with increasing compressibility, which is a direct result of the transverse velocity fluctuation suppression. Finally, the average streamwise and transverse turbulence intensity profiles along with both the normalized primary Reynolds shear stress and the normalized turbulent kinetic energy profiles suggest a reduction in lateral extent on the high-speed side of the mixing layer.

## Acknowledgments

The authors would like to acknowledge the financial support provided by the Office of Naval Research with G. D. Roy as contract monitor and the Air Force Wright Laboratory with A. S. Nejad as contract monitor. In addition, the contributions of graduate assistants Jeff Herrin, Joe Savio, and Paul Rudolph are greatly appreciated.

## References

[1]Brown, G. L., and Roshko, A., "On Density Effects and Large Structures in Turbulent Mixing Layers," *Journal of Fluid Mechanics,* Vol. 64, 1974, pp. 775–816.

[2]Spencer, B. W., "Statistical Investigation of Turbulent Velocity and Pressure Fields in a Two-Stream Mixing Layer," Ph.D. Dissertation, Dept. of Nuclear Engineering, Univ. of Illinois, Urbana, IL, 1970.

[3]Oster, D., and Wygnanski, I., "The Forced Mixing Layer Between Parallel Streams," *Journal of Fluid Mechanics,* Vol. 123, 1982, pp. 91–130.

[4]Bell, J. H., and Mehta, R. D., "Development of a Two-Stream Mixing Layer from Tripped and Untripped Boundary Layers," AIAA Paper 90-0505, Jan. 1990.

[5]Papamoschou, D., and Roshko, A., "The Compressible Turbulent Shear Layer: An Experimental Study," *Journal of Fluid Mechanics,* Vol. 197, 1988, pp. 453–477.

[6]Goebel, S. G., and Dutton, J. C., "Experimental Study of Compressible Turbulent Mixing Layers," *AIAA Journal,* Vol. 29, No. 4, 1991, pp. 538–546.

[7]Elliott, G. S., and Samimy, M., "Compressibility Effects in Free Shear Layers," *Physics of Fluids A,* Vol. 2, No. 7, 1990, pp. 1231–1240.

[8]Clemens, N. T., "An Experimental Investigation of Scalar Mixing in Supersonic Turbulent Shear Layers," Mechanical Engineering Dept., Stanford Univ., HTGL Rept. No. T-274, Stanford, CA, 1991.

[9]Messersmith, N. L., "An Experimental Investigation of Organized Structure and Mixing in Compressible Turbulent Free Shear Layers," Ph.D. Dissertation, Dept. of Mechanical and Industrial Engineering, Univ. of Illinois, Urbana, IL, 1992.

[10]Elliott, G. S., Samimy, M., and Reeder, M. F., "Pressure-Based Real-Time Measurements in Compressible Free Shear Layers," AIAA Paper 90-1980, July 1990.

[11]Shau, Y. R., and Dolling, D. S., "The Detection of Large Scale Structure in Undisturbed and Disturbed Compressible Free Shear Layers," AIAA Paper 90-0711, Jan. 1990.

[12]Sandham, N. D., and Reynolds, W. C., "Three-Dimensional Simulations of Large Eddies in the Compressible Mixing Layer," *Journal of Fluid Mechanics,* Vol. 224, 1991, pp. 133–158.

[13]Leep, L. J., Burr, R. F., and Dutton, J. C., "Three-Dimensional Simulations of Compressible Mixing Layers: Visualizations and Statistical Analysis," *Proceedings of the 1992 ASME Fluids Engineering Conference,* FED-Vol. 133, 1992, pp. 189, 190.

[14]Bogdanoff, D. W., "Compressibility Effects in Turbulent Shear Layers," *AIAA Journal,* Vol. 21, No. 6, 1983, pp. 926, 927.

[15]Papamoschou, D., "Structure of the Compressible Turbulent Shear Layer," *AIAA Journal,* Vol. 29, No. 5, 1991, pp. 680, 681.

[16]McIntyre, S. S., and Settles, G. S., "Optical Experiments on Axisymmetric Compressible Turbulent Mixing Layers," AIAA Paper 91-0623, Jan. 1991.

[17]Ragab, S. A., and Wu, J. L., "Instabilities in the Free Shear Layer Formed by Two Supersonic Streams," AIAA Paper 88-0038, Jan. 1988.

[18]Goebel, S. G., "An Experimental Investigation of Compressible,

Turbulent Mixing Layers," Ph.D. Dissertation, Dept. of Mechanical and Industrial Engineering, Univ. of Illinois, Urbana, IL, 1990.

[19]Bloomberg, J. E., "An Investigation of Particle Dynamics Effects Related to LDV Measurements in Compressible Flows," M.S. Thesis, Dept. of Mechanical and Industrial Engineering, Univ. of Illinois, Urbana, IL, 1989.

[20]Buchhave, P., "Biasing Errors in Individual Particle Measurements with the LDA-Counter Signal Processor," *Proceedings of the LDV-Symposium Copenhagen, The Accuracy of Flow Measurements by Laser Doppler Methods,* Hemisphere, New York, 1975, pp. 258–278.

[21]Gruber, M. R., "Three-Dimensional Velocity Measurements in a Turbulent, Compressible Mixing Layer," M.S. Thesis, Dept. of Aeronautical and Astronautical Engineering, Univ. of Illinois, Urbana, IL, 1992.

[22]Sun, C. C., and Childs, M. E., "A Modified Wall Wake Velocity Profile for Turbulent Compressible Boundary Layers," *Journal of Aircraft,* Vol. 10, No. 6, 1973, pp. 381–383.

[23]Schlichting, H., *Boundary Layer Theory,* 7th ed., McGraw-Hill, New York, 1979, pp. 737, 738.